Proceedings of the 2007 American Control Conference
Marriott Marquis Hotel at Times Square
New York City, USA, July 11-13, 2007

Optimal Placement of a Moving Sensor Network for Track Coverage

K. Baumgartner and S. Ferrari

Abstract— **The problem of optimizing the configuration of a moving sensor network deployed to detect moving targets is formulated using optimal control theory. A cost function of the Lagrange type is obtained through a computational geometry approach to measure the space of line transversals for k of the n sensors by formulating an integral function of the sensors locations, where k is the number of required detections. Then, the cost function is optimized subject to the sensors dynamics expressed by a state-space model. The method is demonstrated for a surveillance application that involves sonobuoys deployed on the ocean's surface to detect underwater targets within a specified region of interest and over a desired period of time. It is shown that a state-space model of the sonobuoy dynamics can be obtained from the steady-state solution of Stokes's problem and a current vector field obtained from oceanographic models or CODAR measurements. In this paper, a solution is presented for the case of non-maneuverable sensors that can be placed anywhere within the region of interest and move subject to the ocean's current. The methodology can also be extended to maneuverable sensors with on-board control capabilities, such as, thrusters, or to acoustic sensors installed on underwater vehicles. The numerical simulations show that by taking into account the drift dynamics the cumulative coverage over a period of seven days can be increased by up to 85%.**

I. INTRODUCTION

Simple, low power sensors distributed throughout an environment can provide situational awareness at a moderate cost. This technology enables military and environmental surveillance tasks [1], such as monitoring ocean features, tracking endangered species, and detecting and tracking underwater vehicles. Many of these sensor implementations require coverage of large regions of interest, where non-cooperative targets whose trajectories are unknown *a priori* must be detected over time. To ensure that the distributed system is both practical and affordable, proximity sensors with individual detection capabilities are often employed to obtain multiple measurements from each track, possibly at different moments in time. Proximity sensors only report a simple energy observation, from which a relative distance measurement from the sensor to the target, referred to as the sensor-to-target closest-point-of-approach (CPA), may be inferred. Multiple sensor detections are used to form a hypothesis for a target's track by fusing the detection events from several sensors in what is referred to as a *track-before-detect* approach [2]. Only after a hypothetical track is formed from a consistent set of k detections, the target is declared detected and tracking capabilities may be deployed.

This work was supported by the Office of Naval Research Young Investigator Program (Code 321).

K. Baumgartner is a graduate student of Mechanical Engineering at Duke University, Durham, NC 27707, USA kac20@duke.edu

S. Ferrari is with Faculty of Mechanical Engineering at Duke University, Durham, NC 27707, USA sferrari@duke.edu

The problem of sensor network coverage as it pertains to detecting a moving target through limited measurements, such as CPA detections, is referred to as *track coverage*. It was first introduced in [3] and formulated using planar geometry. Consequently, the coverage of a network configuration with respect to a pre-defined area of interest can be rapidly assessed by a closed-form function of the sensors positions. The methodology presented in this paper optimizes the time integral of this track-coverage function, and accounts for the dynamics of the sensor networks that are caused by oceanic drift. It has long been recognized in practice that the drift of sonobuoys can have a detrimental impact on the effectiveness of mission objectives, such as detection. The reason is that field integrity is reduced when the local ocean currents create coverage gaps, cluster too many buoys together, or move buoys outside of the coverage area of interest [4]. To minimize the impact that the currents have on the performance of the sonobuoy system, the current vector field is modeled and accounted for by the track-coverage function optimization. One popular approach to measuring ocean currents, referred to as the Lagrangian approach, employs a buoy known as a drifter that rides on the ocean surface and can be tracked by satellite, radar, radio, or sound [5], [6], [7], [8], [9]. Other methods for obtaining current measurements include radar-based measurements, such as Coastal Ocean Dynamics Applications Radar (CODAR) [10], and satellites [11]. In view of these recent technological developments, a methodology is developed for optimally placing a set of proximity sensors whose dynamics are formulated in terms of the surface currents specified by a known vector field.

This paper presents a novel sensor placement problem with the objective of providing maximum track coverage of a rectangular region of interest over time by means of moving sensors. The approach developed in this paper leads to a new problem in dynamic computational geometry pertaining the geometric transversals of moving families of objects. It is shown that a state-space representation of the motions of the individual sensors subject to the current vector field can be derived from sonobuoys oceanic drift models. When the sensor networks have no control capabilities, this method determines the initial sensor positions that will maximize the cumulative track coverage over a specified period of time. When sensors have control capabilities (for example, on-board thrusters), the objective is to determine a suitable control policy that maximizes the cumulative track coverage.

II. Background

A. Track coverage by means of multiple sensors

The problem of target tracking by a sensor network arises in many applications, including surveillance systems, monitoring of endangered species, and manufacturing. As a result, it is receiving considerable attention. Tracking refers to the estimation of the state (e.g., position, velocity, acceleration) of a moving object by means of multiple sensor measurements. Once a detection is declared by sensors in search mode, a target track is formed by estimating its state from the set of measurements acquired over time, through Kalman filtering. In this paper, it is assumed that a central fusion center collects only peak energy information from a set of proximity sensors and then computes all sensor-target distances as shown in [2]. Using only limited sensed information, such as closest-point-of-approach (CPA) detections, it is possible to hypothesize a set of target paths for one or more targets moving at a constant heading and non-zero speed through the sensor field [2].

It is shown in [2] that given a set of τ_i error-free measurements for each of the sensors located at $\mathbf{x} \equiv [\mathbf{x}_1^T \ ... \ \mathbf{x}_i^T \ ... \ \mathbf{x}_n^T]^T$, the target path is a line that is jointly tangent to all circles $C_i(S) \equiv \{\chi : \|\chi - \mathbf{x}_i\| \leq r_i\}$, where $\chi \in \Re^{2\times 1}$, $\|\cdot\|$ is the Euclidean norm, and r_i is the distance from the i^{th} sensor to the target. Figure 1 illustrates two possible tracks formed from two sensor measurements, τ_1 and τ_2. Reliable target detection typically requires two or more individual sensor detections that may be used in a track-before-detect approach.

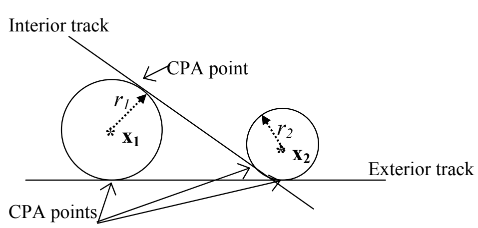

Fig. 1. Geometry of two potential interior and exterior tracks formed by the CPA events for two sensors located at $\mathbf{x}_1$ and $\mathbf{x}_2$ [2]

B. k-Track coverage for a fixed sensor network

The track-coverage optimization problem consists of maximizing the amount of tracks that are intercepted by at least k sensors in a network of n omnidirectional sensors placed in polygonal area $\mathcal{A}$. In [12], this problem was formulated through geometric transversal theory. A set of geometric objects in $\Re^d$ is said to have a *j-transversal* when all objects are intersected by a common j-dimensional flat, such as a track. A function is constructed to measure the space of line transversals for a family of k circles belonging to a set of n circles of different size and location in $\mathcal{A} \in \Re^2$, which here is assumed to be rectangular for simplicity.

Consider a sensor located at $\mathbf{x}_i = [x_{1,i} \quad x_{2,i}]^T$ with a maximum sensor range r_i. Let $\mathbf{v}_i \equiv [x_{1,i} \quad (x_{2,i} - b_{x_2})]^T$ denote the sensor position vector relative to the b-intercept of the x_2-axis. The *coverage cone*, defined as the set of tracks detected by a sensor at $\mathbf{x}_i$ with range r_i, is bounded by the following *high* and a *low* unit vectors,

$$\hat{\mathbf{h}}_i = \begin{bmatrix} \cos\theta_i & -\sin\theta_i \\ \sin\theta_i & \cos\theta_i \end{bmatrix} \frac{\mathbf{v}_i}{\|\mathbf{v}_i\|} = \mathbf{Q}_i^+ \hat{\mathbf{v}}_i \tag{1}$$

and

$$\hat{\mathbf{l}}_i = \begin{bmatrix} \cos\theta_i & \sin\theta_i \\ -\sin\theta_i & \cos\theta_i \end{bmatrix} \frac{\mathbf{v}_i}{\|\mathbf{v}_i\|} = \mathbf{Q}_i^- \hat{\mathbf{v}}_i \tag{2}$$

Where, θ_i denotes half the opening angle of the coverage cone and is easily calculated from $\mathbf{x}_i$ and r_i, because the sensor detection radius forms a right triangle with the low and high position vectors, as shown in [3].

For $n \geq k \geq 1$, the high and low unit vectors of each sensor and b-intercept are ordered according to a positive counterclockwise orientation [13]. Then, the k-coverage cone for the sensors positioned at $(\mathbf{x}_1, ..., \mathbf{x}_k)$ can be defined by the ordered pair $(\hat{\mathbf{l}}^*, \ \hat{\mathbf{h}}^*)$ and is given by,

$$\sin\psi = \|\hat{\mathbf{l}}^* \times \hat{\mathbf{h}}^*\| = \begin{vmatrix} \hat{\mathbf{v}}_\ell^T \mathbf{Q}_\ell^+ \\ \hat{\mathbf{v}}_j^T \mathbf{Q}_j^- \end{vmatrix}, \tag{3}$$

where $|\cdot|$ is the matrix determinant, as shown in [3]. It follows that the track coverage for a rectangular region can be measured by the sum of the opening angles over its borders, that is,

$$\begin{aligned} \mathcal{T}_{\mathcal{A}}^k &= \sum_{b_{x_2}=0}^{L_2} H(\psi)\cdot\psi + \sum_{b_{x_1}=0}^{L_1} H(\zeta)\cdot\zeta \\ &+ \sum_{b_{\chi_2}=0}^{L_2} H(\xi)\cdot\xi + \sum_{b_{\chi_1}=0}^{L_1} H(\rho)\cdot\rho, \end{aligned} \tag{4}$$

where ψ, ζ, ξ, and ρ denote the opening angles of the coverage cones defined with respect to x_2, x_1, χ_2, and χ_1, respectively, and these axis are placed along the four borders of $\mathcal{A}$. $H(\cdot)$ is a heaviside function that ensures that the vector ordering described earlier is guaranteed [3].

When $n > k$, (4) may include overlapping coverage cones, and result into certain tracks being considered more than once by the coverage function. In order to eliminate the possibility for redundant coverage, each of the coverage cones within (4) is formulated using the *principle of inclusion-exclusion* [14], [15]. The resulting function methodically measures the union of possibly non-disjoint sets,

$$\left|\bigcup_{i=1}^{n} A_i\right| = \sum_{j=0}^{n} \left((-1)^{(j+1)} \sum_{S\in I_j} |S| \right), \tag{5}$$

where I_k represents the set of k-fold intersections of members of $C = \{A_1, A_2, ..., A_n\}$. For instance, I_3 contains all possible intersections of three sets chosen from C. S is the union of the j^{th} set combination, and n_α is the total number of set combinations. Therefore, (4) is expanded to

$$2\mathcal{T}_{\mathcal{A}}^k = \sum_{b_{x_2}=0}^{L_2} \sum_{j=1}^{n_\alpha} (-1)^{j+1} \sum_{\psi\in I_j} H(\psi)|\psi|$$

$$+ \sum_{b_{\chi_2}=0}^{L_2} \sum_{j=1}^{n_\alpha} (-1)^{j+1} \sum_{\rho \in I_j} H(\rho)|\rho|$$
$$+ \sum_{b_{x_1}=0}^{L_1} \sum_{j=1}^{n_\alpha} (-1)^{j+1} \sum_{\beta \in I_j} H(\beta)|\beta|$$
$$+ \sum_{b_{\chi_1}=0}^{L_1} \sum_{j=1}^{n_\alpha} (-1)^{j+1} \sum_{\zeta \in I_j} H(\zeta)|\zeta| \qquad (6)$$

Where, the factor of two is used because any track intersecting $\mathcal{A}$ always intersects two of its sides.

The upper bound of (6) represents total coverage, which is provided by a sensor network that detects all tracks in $\mathcal{A}$ at least k times. It is shown in [16] that this upper bound is,

$$\mathcal{T}_{\mathcal{A}}^{\max} = \pi \left(\frac{L_2 + \delta b_{x_2}}{\delta b_{x_2}} + \frac{L_1 + \delta b_{x_1}}{\delta b_{x_1}} \right) \qquad (7)$$

and, thus, it is independent of the number of sensors n or k, and is a function of both the dimensions of $\mathcal{A}$ and the discretization of the reference axes.

III. Track Coverage Problem for a Moving Sensor Network

A moving sensor network, such as one comprised of sonar buoys that are floating due to oceanic drift, develops significant track-coverage holes over time. A coverage hole is defined as a region in parameter space where tracks are not detected by at least k sensors. Another undesirable outcome is the increased redundant coverage, which takes place when more than k sensors detect the same set of tracks. If the sensors have no control inputs, e.g., they are non-maneuverable free-floating sensors, the trajectories of the sensors that maximize the overall coverage over a period of time depend only on the initial conditions. If the sensors can be controlled, e.g., are installed on underwater gliders or are equipped with thrusters, an optimal control policy and trajectory can be obtained from the solution of an optimal control problem. The drift dynamics induced by an oceanic environment are accounted for by utilizing oceanographic models and measurements of the ocean current, which produce a known forcing vector field in the buoy equations of motion [4]. The result is an optimal control problem that seeks to optimize sensor network coverage of an area $\mathcal{A}$, subject to oceanic sensor drift. This paper investigates the problem of optimally placing a set of moving sensors in $\mathcal{A}$ such that their trajectories maximize the network track coverage over a desired period of time. The dynamic sensor network obeys the following assumptions: (*i*) target maintains constant heading and speed; (*ii*) the range of each omnidirectional sensor is known and can be represented by a disk centered at the sensor location; (*iii*) the area of interest is rectangular.

A. Drift Dynamics

The current velocity profile is acquired by oceanographic models [4], satellite [11], or by Coastal Ocean Dynamics Applications Radar (CODAR) [10]. Surface currents can be measured through oceanographic models from *past* measurements acquired from previously deployed buoys in the ocean, as explained in [4]. The measurement of surface currents by CODAR, a high frequency radar system, employs a transmitter that sends out radio waves that scatter off the ocean surface and then return to a receiver antenna. Using this information and the principles of the Doppler shift, CODAR is able to calculate the speed and direction of the surface current.

Another method for obtaining the ocean surface current vector components utilizes state-of-the-art satellite technology. Currently, the most efficient way of deriving the surface currents consists of performing *feature tracking*, which overlaps multiple synthetic aperture radar (SAR) images taken from different satellites over a short period of time [11]. SAR is a side-looking imaging radar that transmits a series of short, coherent pulses to the ground. Then, the high-resolution image is produced by detecting small Doppler shifts to the moving radar. The image-collecting sensors on each satellite have very different dynamic ranges of data, and filtered data with the same dynamic range are essential for feature tracking. The SAR data obtained from different satellites is matched by means of a 2-dimensional band-pass data filter that is localized in both frequency and time, and employs wavelet transforms [11]. For example, Figure 2(a) taken from [11], shows the ocean surface drift (green arrows) derived from the wavelet analysis of two satellites' SAR data over the Luzon Strait near the Philippines (Figure 2(b)).

Once a current vector field has been obtained by one of the above methods, it can be employed in buoy equations of motion that have been validated through experiments in the ocean, and are taken from [4]. The sonobuoy response to a 3-dimensional current profile is represented by a two orthogonal planar current profile characterized by the drag equation

$$D = \frac{1}{2} \rho C_d A V^2 \qquad (8)$$

D is the total drag on a sphere obtained from the steady-state solution to Stoke's Problem along the local current velocity vector. ρ is the fluid density, C_d is the object's coefficient of drag, and A is the object's cross-sectional area. V, the magnitude of the fluid relative velocity vector past the object, has the following components,

$$\Delta \mathbf{v_1} \equiv \mathbf{u_1} - \mathbf{v} \qquad (9)$$
$$\Delta \mathbf{v_2} \equiv \mathbf{v} - \mathbf{u_2}, \qquad (10)$$

assuming that the velocity profile in the vertical direction can be approximated as shown in Figure 3(b). Also, each velocity vector can be described in the plane as $\Delta \mathbf{v_i} = [\Delta v_{x_i} \quad \Delta v_{y_i}]^T$, the water velocity components $\mathbf{u_i} = [u_{x_i} \quad u_{y_i}]^T$, and the sonobuoy velocity components $\mathbf{v} = [v_x \quad v_y]^T$.

In order to describe the sononbuoy velocity by a differential equation,

$$\dot{\mathbf{x}} = \mathbf{v}(t, x, y), \qquad (11)$$

a force balance is applied to the upper and lower spheres that

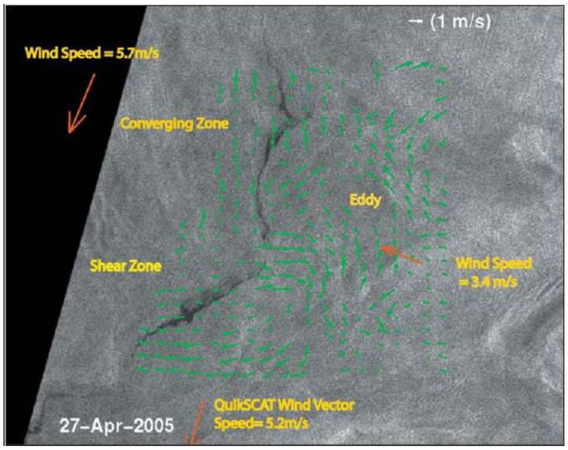

(a)

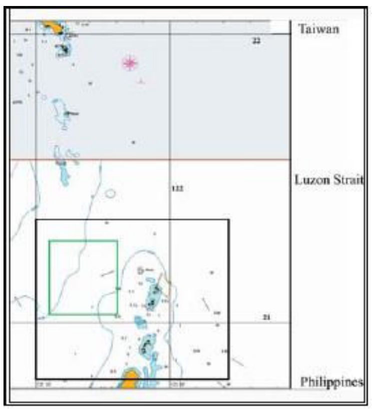

(b)

Fig. 2. (a) Ocean surface drift (green arrows) derived from two satellites' SAR data over the Luzon Strait, and (b) the location map with the SAR image coverage area shown in the large box taken from [11].

approximate the sonobuoy, as shown in Figure 3. It follows that the equations in the x and y directions are:

$$C_{d_1}A_1(\Delta v_{x_1})^2 = C_{d_2}A_2(\Delta v_{x_2})^2 \tag{12}$$

$$C_{d_1}A_1(\Delta v_{y_1})^2 = C_{d_2}A_2(\Delta v_{y_2})^2. \tag{13}$$

Introducing the constant $\beta = \sqrt{(C_{d_2}A_2)/(C_{d_1}A_1)}$, the relative velocities can be written as $\Delta v_{x_1} = \beta\Delta v_{x_2}$ and $\Delta v_{y_1} = \beta\Delta v_{y_2}$. Then, the velocity of the buoy is

$$\mathbf{v} = \begin{bmatrix} \frac{u_{x_1}+\beta u_{x_2}}{1+\beta} \\ \frac{u_{y_1}+\beta u_{y_2}}{1+\beta} \end{bmatrix} \tag{14}$$

Now, let $u_{x_2} = \alpha_x u_{x_1}$ and $u_{y_2} = \alpha_y u_{y_1}$, and for simplicity assume that $\alpha_x = \alpha_y = \alpha$, with $0 \leq \alpha \leq 1$. Then (14) can be written as,

$$\mathbf{v} = \begin{bmatrix} \left(\frac{1+\beta\alpha}{1+\beta}\right) u_{x_1} \\ \left(\frac{1+\beta\alpha}{1+\beta}\right) u_{y_1} \end{bmatrix} = \gamma \begin{bmatrix} u_{x_1} \\ u_{y_1} \end{bmatrix}, \tag{15}$$

with the constant $\gamma \equiv (1+\beta\alpha)/(1+\beta) < 1$. By assuming the buoys move with the surface current, i.e., $\Delta\mathbf{v_i} = 0$, the buoy equation of motion (11) can be simplified to the

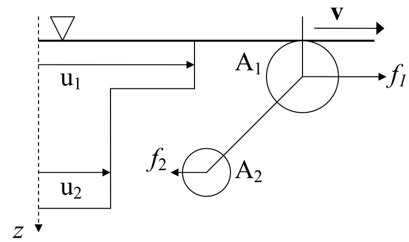

(a)

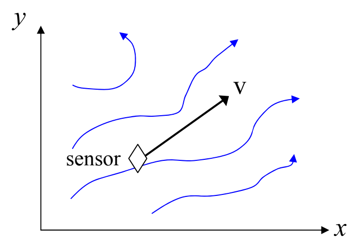

(b)

Fig. 3. (a) The upper and lower components of a sonobuoy in which a force balance of $f_1 = f_2$ is applied, (12)-(13), and (b) is the view from above.

following state space model,

$$\frac{d\mathbf{x}(t)}{dt} = \mathbf{v} = \mathbf{A}\mathbf{x}(t), \tag{16}$$

that is, linear and time-invariant (LTI).

B. Optimal placement of moving sensor networks

The optimization of the track coverage provided by a sensor network over a period of time consists of optimizing the space of line transversals of a moving family of circles. If the sensors are non-maneuverable, the trajectories of the sensors depend only on their initial conditions, namely, their initial positions in $\mathcal{A}$. The coverage function (6) is used to obtain a measure of the cumulative coverage over time in terms of an integral objective function of the Lagrange type. This cost function is derived through a dynamic computational geometry approach that expresses a Lebesgue measure on the space of line transversals in closed form. Since the cost function is not quadratic and is composed of several terms, the solution of this optimal control problem becomes increasingly difficult as $\mathcal{A}$ becomes larger and the number of sensors increases.

When sensors are maneuverable, the objective is to determine a suitable control law that maximizes the cumulative track coverage. For example, the controllable sensor dynamics may be described by the linear ODE

$$\frac{d\mathbf{x}(t)}{dt} = \mathbf{A}\mathbf{x}(t) + \mathbf{G}\mathbf{u}(t). \tag{17}$$

Control power may be introduced to compensate for variations in the drift that would cause the sensor to deviate from its desired trajectory, or to maintain a fixed sensor configuration. The cost function describing the cumulative track coverage in terms of the state and control vectors is

$$\mathcal{J}_{\mathcal{A}}^{k}(\mathbf{x},\mathbf{u},t)=\int_{t_o}^{t_f}\mathcal{T}_{\mathcal{A}}^{k}\{\mathbf{x}(t),\dot{\mathbf{x}}(t),\mathbf{u}(t),t\}dt \tag{18}$$

In this paper, the sensor network is assumed to be governed by (16), and the goal is to find the initial conditions for which the resulting trajectories provide maximum cumulative coverage. Through the dynamic equation (16), the cost function describing the cumulative coverage is formulated in terms of the sensors initial positions. The optimal strategy consists of a set of initial sensor position vectors that maximize the cumulative coverage over a region of interest $\mathcal{A}$. The integrand of the cost function, given by (6), is calculated using the instantaneous high and low unit vectors, $\hat{\mathbf{h}}_i(t=t_i)$ and $\hat{\mathbf{l}}_i(t=t_i)$, that depend on the sensor position vector $\mathbf{x}(t_i)$, as shown in (1) and (2). When applied to a moving sensor network that is not maneuverable, the cost function simplifies to

$$\mathcal{J}_{\mathcal{A}}^{k}(\mathbf{x},t)=f(\mathbf{x},\dot{\mathbf{x}})=\int_{t_o}^{t_f}\mathcal{T}_{\mathcal{A}}^{k}[\mathbf{x}_1(t),...,\mathbf{x}_n(t)]dt. \tag{19}$$

Since the governing equation (16) is linear, the sensor positions $\mathbf{x}(t)$ can be related to their initial positions by the transition matrix, $\mathbf{\Phi}(t,t_o)$:

$$\mathbf{x}(t)=\mathbf{\Phi}(t,t_o)\mathbf{x}(t_o). \tag{20}$$

Where, $\mathbf{\Phi}=e^{\mathbf{A}(t-t_o)}$, and the elements of $\mathbf{A}$ are constant parameters obtained from the known current vector field. A general form for $\mathbf{\Phi}(t,t_o)$ is derived in Section III-C . Then, (20) is substituted in (19), and the integral is maximized with respect to $\mathbf{x}(t_o)=\mathbf{x}_o$ in order to obtain the optimal initial position, $\mathbf{x}_o^*$.

The optimization problem of maximizing the cumulative coverage, $\mathcal{J}$, for n sensors and k-required sensor detections is constrained such that the initial sensors locations (*i*) prevent range overlap and (*ii*) are contained within $\mathcal{A}$, where $\mathcal{A}$ is an $L_1\times L_2$ rectangle. Thus, the optimization problem becomes,

$$\max_{\mathbf{x}_o}\mathcal{J}_{\mathcal{A}}^{k},\quad \text{subject to } \mathbf{x}(t)=\mathbf{\Phi}(t,t_o)\mathbf{x}(t_o) \tag{21}$$

and subject to (*i*)-(*ii*). In order to solve (21) for the initial sensor positions, the Matlab function *fmincon* is implemented to maximize the integral function (19) with respect to $\mathbf{x}_o$.

C. Example: Optimization of Dynamic Track Coverage for $n=k=1$

A simple example with $n=1$ sensor and $k=1$ is presented in order to illustrate the solution approach outlined in the previous section. $\mathbf{\Phi}$ is derived for a general state-space matrix $\mathbf{A}$ representing the vector field and can easily be applied to $n>1$ by increasing the dimensions appropriately. Assuming the buoys moves in a linear fashion with the surface current according to (16), $\mathbf{A}$ is a $2n\times 2n$ matrix that for one sensor can be defined as,

$$\mathbf{A}=\begin{bmatrix} a & b\\ c & d\end{bmatrix}, \tag{22}$$

where the elements of $\mathbf{A}$ are obtained from the current vector field, as explained in Section III-A. The trajectory of one sensor can be described in terms of the initial sensor position using (20) as follows

$$\dot{\mathbf{x}}=\mathbf{A}\mathbf{\Phi}(t,t_o)\mathbf{x_o} \tag{23}$$

The eigenvalues, or roots, of the characteristic equation $\det(s\mathbf{I}-\mathbf{A})$ are found to be,

$$\lambda_1 = \frac{K_1+\sqrt{K_1^2-4\cdot K_2}}{2} \tag{24}$$

$$\lambda_2 = \frac{K_1-\sqrt{K_1^2-4\cdot K_2}}{2} \tag{25}$$

where $K_1=d+a$ and $K_2=ad-bc$. Therefore, the transition matrix becomes,

$$\mathbf{\Phi}(t,0)=\begin{bmatrix}(c_1e^{\lambda_1 t}+c_2e^{\lambda_2 t}) & (c_3e^{\lambda_1 t}+c_4e^{\lambda_2 t})\\ (c_5e^{\lambda_1 t}+c_6e^{\lambda_2 t}) & (c_7e^{\lambda_1 t}+c_8e^{\lambda_2 t})\end{bmatrix}. \tag{26}$$

Because $\mathbf{\Phi}(0,0)=\mathbf{I}$ and $\dot{\mathbf{\Phi}}(0,0)=\mathbf{A}$, a system of eight simultaneous equations is used to obtain the eight unknowns in $\mathbf{c}=[c_1,...,c_8]^T$ in terms of the constants a, b, c, d, λ_1, and λ_2, as shown in Table I.

TABLE I
THE CONSTANTS OF $\mathbf{\Phi}$

$c_1=\frac{a-\lambda_2}{\lambda_1-\lambda_2}$	$c_3=\frac{b}{\lambda_1-\lambda_2}$	$c_5=\frac{c}{\lambda_1-\lambda_2}$	$c_7=\frac{d-\lambda_2}{\lambda_1-\lambda_2}$
$c_2=\frac{a-\lambda_1}{\lambda_2-\lambda_1}$	$c_4=\frac{b}{\lambda_2-\lambda_1}$	$c_6=\frac{c}{\lambda_2-\lambda_1}$	$c_8=\frac{d-\lambda_1}{\lambda_2-\lambda_1}$

Substituting the values in Table I into (26), and substituting (26) into (23), the optimal initial conditions can be obtained by maximizing the resulting integral function (19). For example, for one sensor, the integrand of the cost function (19) simplifies through the relationship $\sin\theta=r/\|\mathbf{v}\|$,

$$\begin{aligned}\mathcal{J}_{\mathcal{A}}^{k=1} = {} & \frac{1}{2}\int_0^{t_f}\Bigg[\sum_{b_{x_2}=0}^{L_2}\frac{r}{\|\mathbf{v}(t)\|_{x_2}}+\sum_{b_{x_1}=0}^{L_1}\frac{r}{\|\mathbf{v}(t)\|_{x_1}}\\ & +\sum_{b_{\chi_2}=0}^{L_2}\frac{r}{\|\mathbf{v}(t)\|_{\chi_2}}+\sum_{b_{\chi_1}=0}^{L_1}\frac{r}{\|\mathbf{v}(t)\|_{\chi_1}}\Bigg]dt,\end{aligned} \tag{27}$$

where $\|\mathbf{v}\|$ is the position vector relative to the axes indicated by the subscript, for example, $\|\mathbf{v}(t)\|_{x_1}=\sqrt{(x_1-b_{x_1})^2+x_2^2}$.

IV. Results and Applications

The methodology developed in this paper is used to optimize the track coverage of a moving sensor network with respect to an area of interest over a period of time. This problem is relevant to sensor networks floating and drifting in the ocean subject to the surface currents that are employed for detecting moving targets in a region of interest. A cumulative track coverage function is presented in Section III-B and is optimized subject to the drift dynamics described in Section III-A. The $(k = 3)$ - track coverage of a network with $n = 10$ sensors, and ranges $r = [3,\ 3,\ 5,\ 5,\ 6,\ 6,\ 8,\ 8,\ 10,\ 10]^T$, is considered. The parameter k represents the number of CPA detections that are required for declaring a track detected. For comparison, the sensors are first placed according to the optimization of the static coverage function (6), without accounting for the buoys dynamics, as shown in blue in in Figure 4. When the cumulative track coverage function (19) is optimized subject to the drift dynamics (16), the sensor network is deployed at the positions shown in red in Figure 4. The resulting sensors trajectories, plotted in Figures 5(a) and 5(b), differ significantly due to the diversity in the ocean currents that are experienced by the individual sensors. Consequently, the track coverage of the two sensor networks also differs significantly.

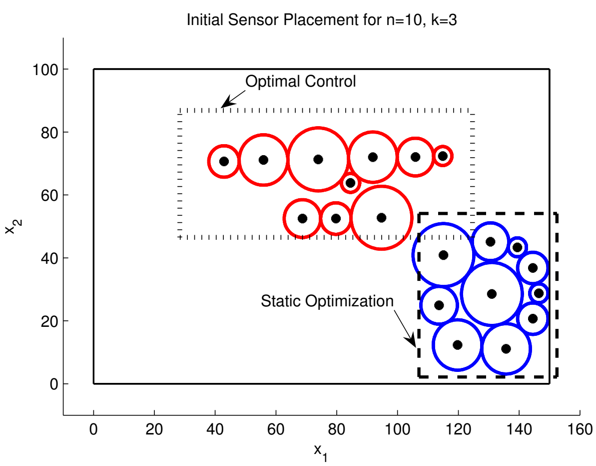

Fig. 4. Comparing the initial sensor configurations by maximizing the static and optimal control coverage equations, (6) and (19), respectively.

The time histories of the track coverage provided by the drifting sensor networks are plotted in Fig. 6. Although the two sensor networks are comprised of the same number of sensors and of the same individual performance (range), the different placement results in significantly different drift patterns for the sensors over the 7-days mission (Figure 5). Consequently, it can be seen from Fig. 6 that the coverage provided by the sensors placed by optimizing the cumulative coverage function is much improved over time, despite the initial coverage being higher for the network placed by the static optimization. The maximum coverage provided by the sensor network placed by optimal control peaks at approximately 6 days, and displays a 43% decrease in coverage from initial deployment to the end of the mission. Whereas, the sensor network placed according to the static optimization peaks initially, but then decreases by 86% over the 7-days period. Finally, the cumulative coverage (Fig. 6) reveals a 85% increase as a result of the initial placement accounting for the drift dynamics.

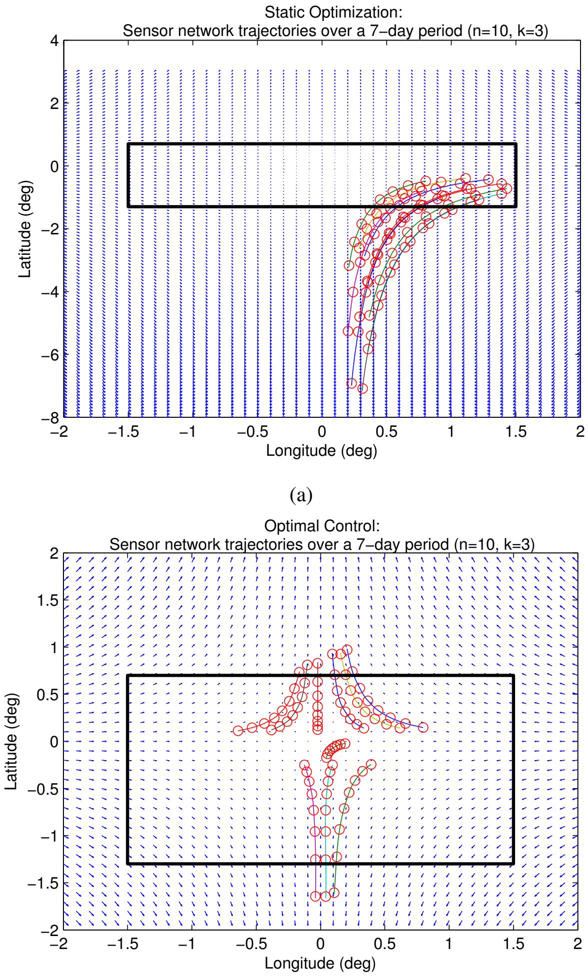

(a)

(b)

Fig. 5. For $n = 10$, $k = 3$ and mission time of 7 days, the drift trajectories of sensors placed according to maximizing (a) the static coverage equation (6) and (b) the optimal control coverage equation (19).

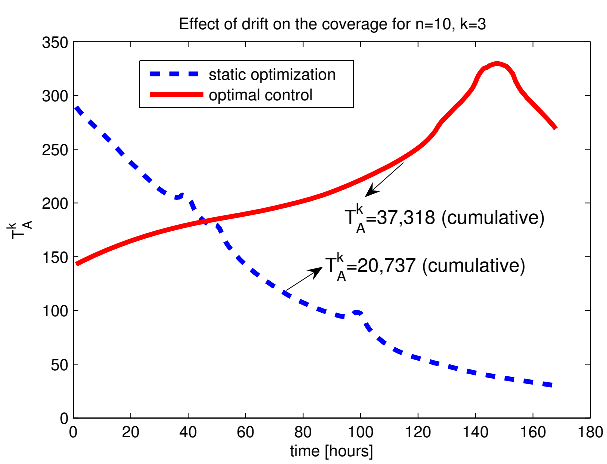

Fig. 6. Coverage deterioration for sensors placed according to the optimal control and static coverage equations.

V. Conclusions

An approach is presented for formulating and optimizing track coverage in moving sensor networks that are required to operate over an extended period of time. The approach is applicable to proximity sensor networks that are implemented for the purpose of detecting and tracking moving targets through limited measurements, such as CPA detections. The approach is based on the formulation of a novel optimal control problem in computational geometry. In this paper, the sensors are assumed to have known and constant ranges and to move according to linear governing equations that include knowledge of the ocean currents, as obtained by CODAR or satellite. The advantage of deploying the sensors according to their projected drift trajectories is demonstrated through simulations involving 10 sensors and $k = 3$ required detections. The results show that the coverage provided by the moving sensor network is much improved with respect to when the sensors are deployed simply by optimizing their initial configuration without accounting for the dynamic environment.

VI. Acknowledgments

This work was supported by the Office of Naval Research Young Investigator Program (Code 321).

References

[1] V. Isler, S. Khanna, J. Spletzer, and C. Taylor, "Target tracking with distributed sensors: The focus of attention problem," *Computer Vision and Image Understanding*, vol. 100, pp. 225–247, 2005.

[2] T. A. Wettergren, R. L. Streit, and J. R. Short, "Tracking with distributed sets of proximity sensors using geometric invariants," *IEEE Transactions on Aerospace and Electronic Systems*, vol. 40, no. 4, pp. 1366–1374, October 2004.

[3] S. Ferrari, "Track coverage in sensor networks," *Proceedings of the ACC 2006*, pp. 1–10, 2006.

[4] D. Hammond, "Sonobuoy field drift prediction," *Technical Report: Naval Air Warfare Center Aircraft Division*, 13 January 2005.

[5] H. Freeland, P. Rhines, and T. Rossby, "Eddy resolution versus eddydiffusion in a double gyre gcm. part ii: Mixing of passive tracers," *Journal of Phys. Oceanography*, vol. 24, pp. 387–402, 1975.

[6] W. Krauss and C. Boning, "Lagrangian properties of eddy fields in the northern atlantic as deduced from satellite-tracked buoys," *Journal of Mar. Res.*, vol. 45, pp. 259–291, 1987.

[7] V. Rupola, B. Hua, A. Provenzale, and V. Artale, "Lagrangian velocity spectra at 700 m in the western north atlantic," *J. Phys. Oceanog.*, vol. 26, pp. 1591–1607, 1996.

[8] R. E. Davis, "Lagrangian ocean studies," *Annual Reviews of Fluid Mechanics*, vol. 23, pp. 43–64, 1991.

[9] W. B. Wilson, "Numerical modeling of drifting buoys and its relevence to lagrangian tracking," *Engineering Structures*, vol. 23, pp. 885–901, 2001.

[10] *COOL, Rutgers University*, p. http://marine.rutgers.edu/, 2002.

[11] A. Liu, Y. Zhao, and M.-K. Hsu, "Ocean surface drift revealed by synthetic aperture radar images," *EOS*, vol. 87, no. 24, pp. 233–239, 13 June 2006.

[12] J. Goodman, R. Pollack, and R. Wenger, "Geometric transversal theory," in *New Trends in Discrete and Computational Geometry*, J. Pach, Ed. Springer Verlag, 1991, pp. 163–198.

[13] S. J. Colley, *Vector Calculus*, 3rd ed.

[14] S. Ross, *Introduction to Stochastic Dynamic Programming*. Academic Press, 1983.

[15] J. Pitman, *Probability*. Springer-Verlag, 1993.

[16] K. A. C. Baumgartner and S. Ferrari, "Geometric transversal approach to analyzing track coverage in sensor networks," submitted to *IEEE Trans. on Mobile Computing*, 2007.